Title

GPCR signaling regulates severe stress-induced organismic death in Caenorhabditis elegans

Journal

Aging Cell, 22(1)

ISSN

1474-9718

Authors

Wang, Changnan
Long, Yong
Wang, Bingying
et al.

Publication Date

2023

DOI

10.1111/acel.13735

Peer reviewed

Received: 3 July 2022 | Revised: 5 October 2022 | Accepted: 10 October 2022

DOI: 10.1111/acel.13735

Aging Cell WILEY

RESEARCH ARTICLE

GPCR signaling regulates severe stress-induced organismic death in *Caenorhabditis elegans*

Changnan Wang[1,2] | Yong Long[3] | Bingying Wang[2] | Chao Zhang[1] | Dengke K. Ma[2,4]

[1]Department of Plastic and Reconstructive Surgery, Shanghai Ninth People's Hospital, Shanghai Jiao Tong University School of Medicine, Shanghai, China

[2]Cardiovascular Research Institute and Department of Physiology, University of California San Francisco, San Francisco, California, USA

[3]State Key Laboratory of Freshwater Ecology and Biotechnology, Institute of Hydrobiology, Chinese Academy of Sciences, Wuhan, China

[4]Innovative Genomics Institute, University of California, Berkeley, California, USA

Correspondence
Chao Zhang, Department of Plastic and Reconstructive Surgery, Shanghai Ninth People's Hospital, Shanghai Jiao Tong University School of Medicine, Shanghai, China.
Email: zhangchao@shsmu.edu.cn

Dengke K. Ma, Cardiovascular Research Institute and Department of Physiology, University of California San Francisco, San Francisco, CA, USA.
Email: dengke.ma@ucsf.edu

Funding information
David and Lucile Packard Foundation; National Institute of General Medical Sciences; National Institutes of Health; National Natural Science Foundation of China

Abstract

How an organism dies is a fundamental yet poorly understood question in biology. An organism can die of many causes, including stress-induced phenoptosis, also defined as organismic death that is regulated by its genome-encoded programs. The mechanism of stress-induced phenoptosis is still largely unknown. Here, we show that transient but severe freezing-thaw stress (FTS) in *Caenorhabditis elegans* induces rapid and robust phenoptosis that is regulated by G-protein coupled receptor (GPCR) signaling. RNAi screens identify the GPCR-encoding *fshr-1* in mediating transcriptional responses to FTS. FSHR-1 increases ligand interaction upon FTS and activates a cyclic AMP-PKA cascade leading to a genetic program to promote organismic death under severe stress. FSHR-1/GPCR signaling up-regulates the bZIP-type transcription factor ZIP-10, linking FTS to expression of genes involved in lipid remodeling, proteostasis, and aging. A mathematical model suggests how genes may promote organismic death under severe stress conditions, potentially benefiting growth of the clonal population with individuals less stressed and more reproductively privileged. Our studies reveal the roles of FSHR-1/GPCR-mediated signaling in stress-induced gene expression and phenoptosis in *C. elegans*, providing empirical new insights into mechanisms of stress-induced phenoptosis with evolutionary implications.

1 | INTRODUCTION

Organisms of all life forms on earth live with varying but limited lifespans. While the natural aging process and regulation of lifespan in many different organisms have been extensively studied (Antebi, 2007; Fontana & Partridge, 2015; Kenyon, 2010; López-Otín et al., 2013; Mutlu et al., 2021; Shore & Ruvkun, 2013), little is known about how a multicellular organism dies at the end of its life after normal aging or in the middle of its life. In nature, the death of an organism can have various causes, including severe abiotic stresses (e.g., heat or starvation), pathogens or predators from ever-changing environments. Prolonged severe abiotic stresses can lead to death of organisms, in many cases likely because of failure in adapting to the stress, or alternatively through stress-induced phenoptosis (Longo

et al., 2005; Skulachev, 1999; Skulachev, 2002; Skulachev, 2019). Using the nematode *C. elegans* as a model organism, we have previously discovered that severe stress from cold shock (CS) followed by warming promotes phenoptosis through a gene transcriptional pathway (Jiang et al., 2018). Discovery of such rapid thermal stress-induced phenoptosis and the genetic tractability of *C. elegans* afford unprecedented access and opportunities to identify the underlying cell signal transduction pathway and mechanisms of stress-induced phenoptosis.

With its small body size, *C. elegans* experiences varying temperatures depending on the ambient environment and exhibits stereotypic behavioral and cell physiological response to chronic or acute mild (10-15 °C) hypothermia (Al-Fageeh & Smales, 2006; Garrity et al., 2010; Xiao et al., 2013). *C. elegans* can live and reproduce normally within 15–25 °C and increases lifespan when grown under chronic mild hypothermia (15 °C) (Lee et al., 2019; Xiao et al., 2013). Temperature beyond this range causes stress, sterility, and organismic death. By studying *C. elegans* mutants abnormally responding to severe thermal (4 °C CS, recovery at 20 °C) stress stimuli, we identified ZIP-10, a bZIP-type transcription factor that promotes severe thermal stress-induced genes and phenoptosis (Jiang et al., 2018). We showed that ZIP-10 activates a genetic program and up-regulates protease-encoding genes in intestinal cells to promote phenoptosis (Jiang et al., 2018). Both the cold-induced *zip-10* expression and the death-promoting effect of ZIP-10 appeared more prominent in old adults than larvae (Jiang et al., 2018).

We postulate that genetic programs underlying stress-induced phenoptosis may have evolved because of antagonistic pleiotropic effects and/or "kin selection" at the population level so that the phenoptosis of adult and weak individuals after severe cold-thermal stress would benefit less stressed and reproductively more privileged ones to facilitate the spreading of genes by fit individuals under resource-limiting and high-stress conditions (Hamilton, 1963; Jiang et al., 2018; Smith, 1964). While evolutionary mechanisms and significance of phenoptosis remain debatable in the field (Galimov et al., 2019; Kirkwood & Melov, 2011; Longo et al., 2005; Sapolsky, 2004; Skulachev, 2019), many empirical studies suggest that organisms with clonal population structures such as *C. elegans* may indeed chronically age or die under stresses by mechanisms (terminal investment, antagonistic pleiotropy, consumer sacrifice, or disposable soma) that can benefit the progeny or reproductive success of the organism itself (Ezcurra et al., 2018; Galimov & Gems, 2020; Gulyas & Powell, 2021; Wu et al., 2022).

Despite critical roles of ZIP-10 in cold-thermal stress-induced phenoptosis in *C. elegans*, its upstream regulators linking severe stress to the ZIP-10-dependent genetic program remains unidentified. By transcriptome profiling, RNAi screens, and genotype-to-phenotype mechanistic analysis, we uncovered a GPCR (FSHR-1, follicular stimulating hormone receptor-related) cascade that activates ZIP-10-dependent transcriptional response to freeze–thaw stress (FTS). Activation of this pathway promotes organismic phenoptosis under severe FTS conditions, more prominently in adults than young larval animals. Our findings reveal an essential role of FSHR-1 and its GPCR signaling cascade in stress-induced gene expression, providing a mechanistic understanding of stress-inducphenoptosis and empirical evidence with implications for the evolutionary kin selection theory and the "disposable soma" hypothesis of organismic aging.

2 | RESULTS

2.1 | RNAseq identifies transcriptomic changes to freeze–thaw stress in *C. elegans*

By exploring various severe hypothermic conditions in *C. elegans*, we identified an environmental stress scheme (−20 °C freezing for 45 min followed by recovery at 20 °C for 24 h, FTS) that triggers robust ZIP-10-dependent phenoptosis with higher penetrance than a previous scheme using a 4 °C cold shock (Jiang et al., 2018) (Figure 1a). We measured the survival rates of both wild type and *zip-10* mutants to quantify organismic phenoptosis under such scheme for *C. elegans* at different developmental stages (larval L1, L4, young and older adults). We found that wild-type animals exhibited progressively increased rates of FTS-induced death along with age, with the young (48 h post-L4) and older adult-stage (5 days post L4) populations reaching nearly 100% death rates after FTS treatment while many larvae survived (Figure 1b). By contrast, FTS-induced phenoptosis was markedly attenuated in *zip-10* mutants, particularly at young adult stages. Given the role of ZIP-10 in organismic death and its regulation by severe cold-thermal stress conditions (Jiang et al., 2018) (and see below), we refer to such severe cold/freezing thermal stress-induced organismic deaths as phenoptosis for simplicity (yet mechanistically do not distinguish between active killing and increased sensitivity). These results establish a robust FTS scheme to induce rapid and environmental stress-triggered phenoptosis in *C. elegans* and also confirm a critical role of ZIP-10 in severe cold/freezing thermal stress-induced phenoptosis.

To identify genes acutely regulated by FTS in *C. elegans* that may participate in phenoptosis, we conducted RNA sequencing (RNAseq) of wild-type *C. elegans* populations after 25-min exposure to −20 °C freezing followed by recovery at 20 °C for 1 h. We used this regime to identify genes that specifically and rapidly respond to FTS rather than those that respond to general organismic deterioration once phenoptosis occurs. After differential expression analyses of triplicate samples, we identified 277 genes that are significantly up- or down-regulated by FTS conditions (Figure 1c,d). Tissue enrichment analysis (TEA, Wormbase) revealed that the intestine is the most prominent site of gene regulation by FTS (Figure S1a). FTS-regulated genes do not overlap apparently with those regulated by common stress-responding transcription factors DAF-16 (nutritional stress), SKN-1 (oxidative stress), HSF-1 (heat stress), or HIF-1 (hypoxic stress), and are involved in biological processes including lipid remodeling (e.g. *oac-31*, *oac-14*, and *oac-6*), responses to abiotic and pathogen stresses (e.g. *kreg-1*, *irg-1* and *lys-3*) (Figure S1b-d). We generated transgenic *C. elegans* strains in which GFP is driven by promoters

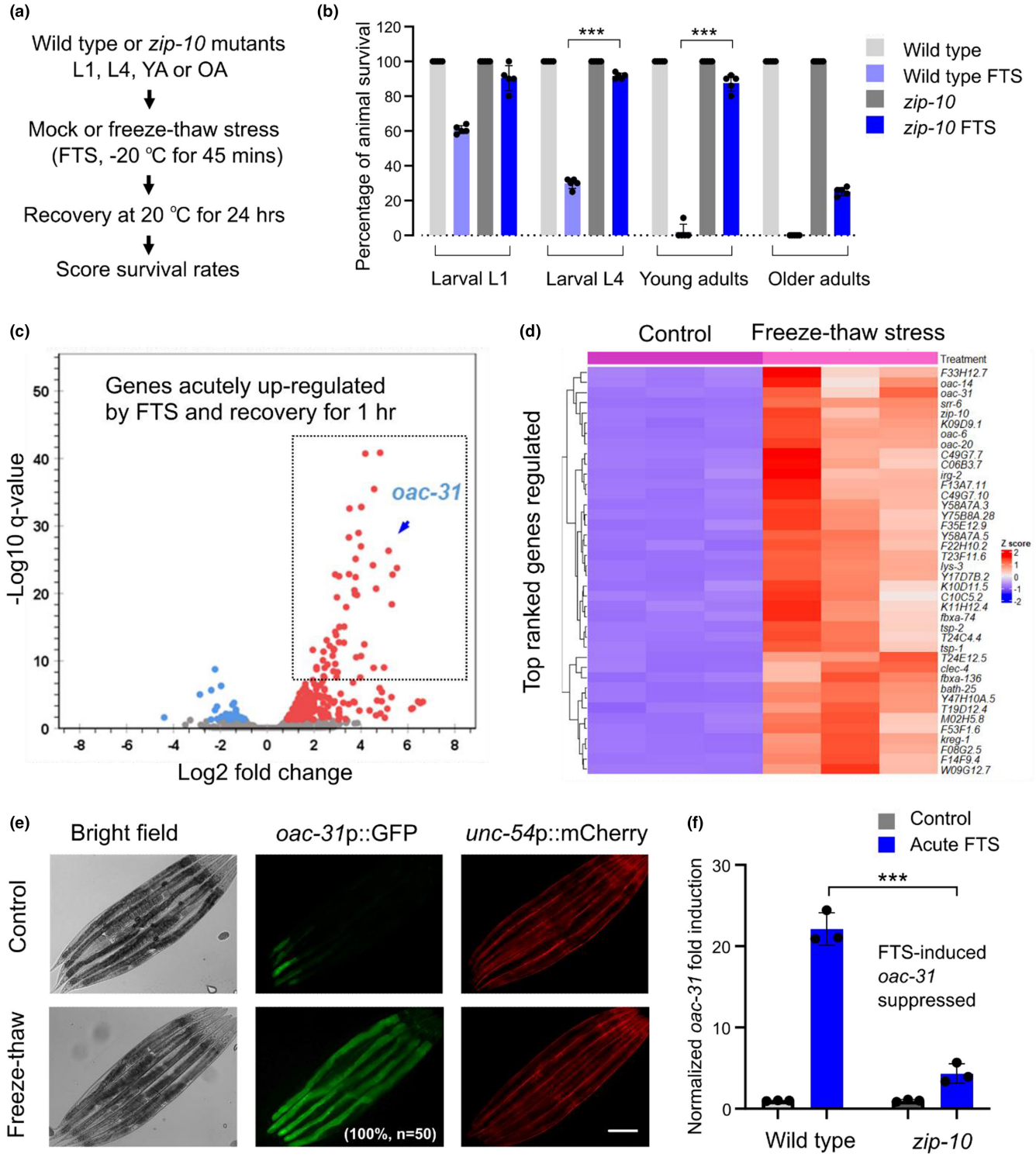

FIGURE 1 RNAseq identifies transcriptomic changes to freeze–thaw stin *C. elegans*. (a), schematic of experimental flow to assay FTS-induced phenoptosis. (b), quantification of phenoptosis based on percentages of animals that survived after FTS in each condition (young adults, 2 days post L4; older adults, 5 days post L4). Values are means ± S.D with $^{***}p < 0.001$ (one-way ANOVA with post hoc Tukey HSD, N = 5 independent experiments, n > 50 for each experiment). (c), volcano plot showing identified genes that are regulated by FTS based on RNAseq. Red: Up-regulated. Blue: Down-regulated. (d), heat map and hierarchical clustering analysis showing the top 50-ranked genes regulated by FTS. (e), representative epifluorescence images showing *oac-31*p::GFP but not co-injection marker *unc-54*p::mCherry induction by FTS. (f), qRT-PCR showing induction of endogenous *oac-31* by FTS in wild type but attenuated in *zip-10(ok3462)* loss-of-function mutants. Values are means ± S.D with $^{***}p < 0.001$ (two-way ANOVA for genotype-effect interaction and post hoc Tukey HSD, N = 3 independent experiments, n > 50 for each experiment). Scale bar, 100 μm

of the top-ranked FTS-inducible genes. *oac-31*p::GFP emerged as a robust FTS-inducible reporter with a low baseline expression and high-fold high-penetrance induction by FTS (Figure 1e). We confirmed by quantitative RT-PCR (qRT-PCR) that FTS up-regulates endogenous *oac-31* in a ZIP-10 dependent manner (Figure 1f). *oac-31* encodes a *C. elegans* homolog of sterol O-acyltransferases and is also the most up-regulated member among the *oac* gene family (Figure S1g). These results identify transcriptomic changes to FTS and led to *oac-31*p::GFP as a robust transcriptional reporter for the genetic response to FTS.

2.2 | RNAi screens identify FSHR-1/GPCR signaling in regulating responses to FTS

With an integrated *oac-31*p::GFP transgenic reporter strain, we performed RNAi (Figure 2a) and forward genetic screens to identify genes that are required for FTS induction of *oac-31*p::GFP. For the RNAi screen, we assembled a library of RNAi clones that target genes with adequate intestinal expression (Transcript per million reads, TPM > 2.0) and encoding transmembrane receptors or transcription factors representing a comprehensive set of signal transduction pathways in *C. elegans* (Table S1; Figure S2a). We found that two gene RNAi clones (*sbp-1* and *tra-1*) activated baseline *oac-31*p::GFP, whereas the other two gene RNAi clones (*fshr-1* and *zip-10*) decreased FTS-induced *oac-31*p::GFP (Figure S2b,c). *fshr-1* encodes a glycoprotein hormone receptor homolog in *C. elegans* and has been implicated in mediating oxidative and innate immune responses (Cho et al., 2007, p.1; Kim & Sieburth, 2020, p.; Powell et al., 2009; Miller et al., 2015; Kudo et al., 2000). A genetic deletion allele *ok778* (backcrossed to N2 for 5 times) of *fshr-1* fully recapitulated the RNAi phenotype in blocking FTS-induced *oac-31*p::GFP (Figure 2b). Neither FTS nor *fshr-1* RNAi affected *unc-54*p::mCherry, the transgenic co-injection marker for *oac-31*p::GFP. By qRT-PCR, we confirmed that FTS induction of *oac-31* (and also another gene *ncr-1* identified from RNAseq) requires *fshr-1* (Figure S2d). However, at least two other genes, *W09G12.7*, and *tsp-1* do not require *fshr-1* for induction by FTS (Figure S2e). These results reveal the essential and specific role of *fshr-1* in transcriptional up-regulation of FTS-induced genes including *oac-31*.

fshr-1 encodes the sole ortholog of glycoprotein hormone receptor family proteins in the *C. elegans* genome (Cho et al., 2007; Kudo et al., 2000). FSHR-1 family proteins are GPCRs that couple to the small G-protein Gαs to stimulate cAMP production and downstream protein kinase A (PKA) signaling. We found that a gain-of-function (GOF) mutation (Schade et al., 2005) in the *C. elegans* Gαs gene *gsa-1* strongly activated *oac-31*p::GFP in the intestine even without FTS (Figure 2c). GOF of the Gαs GSA-1 leads to cAMP elevation and activation of PKA, which comprises the catalytic subunit KIN-1 and the inhibitory regulatory subunit KIN-2 in *C. elegans* (Lu et al., 1990). We found that *kin-2* RNAi led to constitutive *oac-31*p::GFP activation as *gsa-1* GOF did (Figure 2d), and both phenotypes can be suppressed by *kin-1* but not *fshr-1* RNAi (Figure 2e). These results indicate that FTS up-regulates *oac-31* via a classic FSHR-1/GPCR-mediated cAMP and KIN-1/PKA signaling cascade (Figure 2f).

2.3 | FSHR-1 acts in the intestine to regulate ZIP-10 and cold-induced phenoptosis

We next examined the site of expression/action of FSHR-1 and its physiological consequences in FTS-induced phenoptosis. A transcriptional reporter with GFP driven by the promoter of *fshr-1* revealed its predominant intestinal site of expression (Figure 3a). A translational reporter with mCherry driven by the promoter and the genomic protein-coding sequence of *fshr-1* also revealed an intestinal pattern of FSHR-1::mCherry (Figure 3b). Transgenic wild-type *fshr-1* driven by the intestine-specific *ges-1* promoter rescued *oac-31* induction by FTS in *fshr-1* mutants, whereas RNAi against *fshr-1* specifically in the intestine nearly abolished *oac-31* induction by FTS (Figure 3c). FTS-induced *oac-31* also requires *zip-10* (Figure 1f), consistent with its role in mediating transcriptional responses to cold stress in intestinal cells. Furthermore, we found that FTS strongly induced *zip-10* expression itself in control RNAi but not intestine-specific *fshr-1* RNAi-treated animals (Figure 3d). Although FTS transcriptionally up-regulates *zip-10* through FSHR-1, high baseline expression of ZIP-10 likely also contributes to *oac-31* expression given its induction kinetics. These results indicate that FSHR-1 acts in the intestine to promote FTS-induced *zip-10* and *oac-31* gene expression.

We next assessed the role of the FSHR-1 signaling cascade in FTS-induced phenoptosis. Compared with the wild type, *fshr-1* loss-of-function mutants showed increased rates of survival after FTS for both larvae and adults (Figure 3e). We observed death-characteristic blue fluorescence after the FTS treatment in wild-type adult animals as previously reported for naturally dying animals (Coburn et al., 2013), but markedly less so in *zip-10* or *fshr-1* mutants (Figure 3f). In addition, FLR-2 is the sole *C. elegans* ortholog of glycoprotein hormones and putative FSHR-1 ligand (Oishi et al., 2009, p.2) that may signal through the FSHR/GSA-1/PKA cascade (Figure 2). Like *fshr-1* deficient animals, loss of *flr-2* or *kin-1* caused defective *oac-31* induction by FTS (Figure 4a). To determine the epistatic relationship of the genes in the FLR-2/FSHR-1 pathway for FTS-induced phenoptosis, we examined how their loss-of-function or gain-of-function impacted FTS-induced phenoptosis at L4 stages, in which either positive or negative effects on phenoptosis can be quantitatively measured (Figure 4b). Both *flr-2* single and *flr-2; fshr-1* double loss-of-functions (by mutant or RNAi) showed defective FTS-induced phenoptosis (Figure 4b). Consistent with their roles in the regulation of *oac-31* downstream of FSHR-1, *gsa-1* gain-of-function, or *kin-2* loss-of-function exhibited enhanced FTS-induced phenoptosis, while such enhancement can be suppressed with *zip-10* loss-of-function mutations (Figure 4b). Loss of ZIP-10 strongly attenuated FTS-induced phenoptosis (Figure 1a), while individual loss of its target genes *oac-31* or *asp-17* (previously identified as a ZIP-10-dependent gene

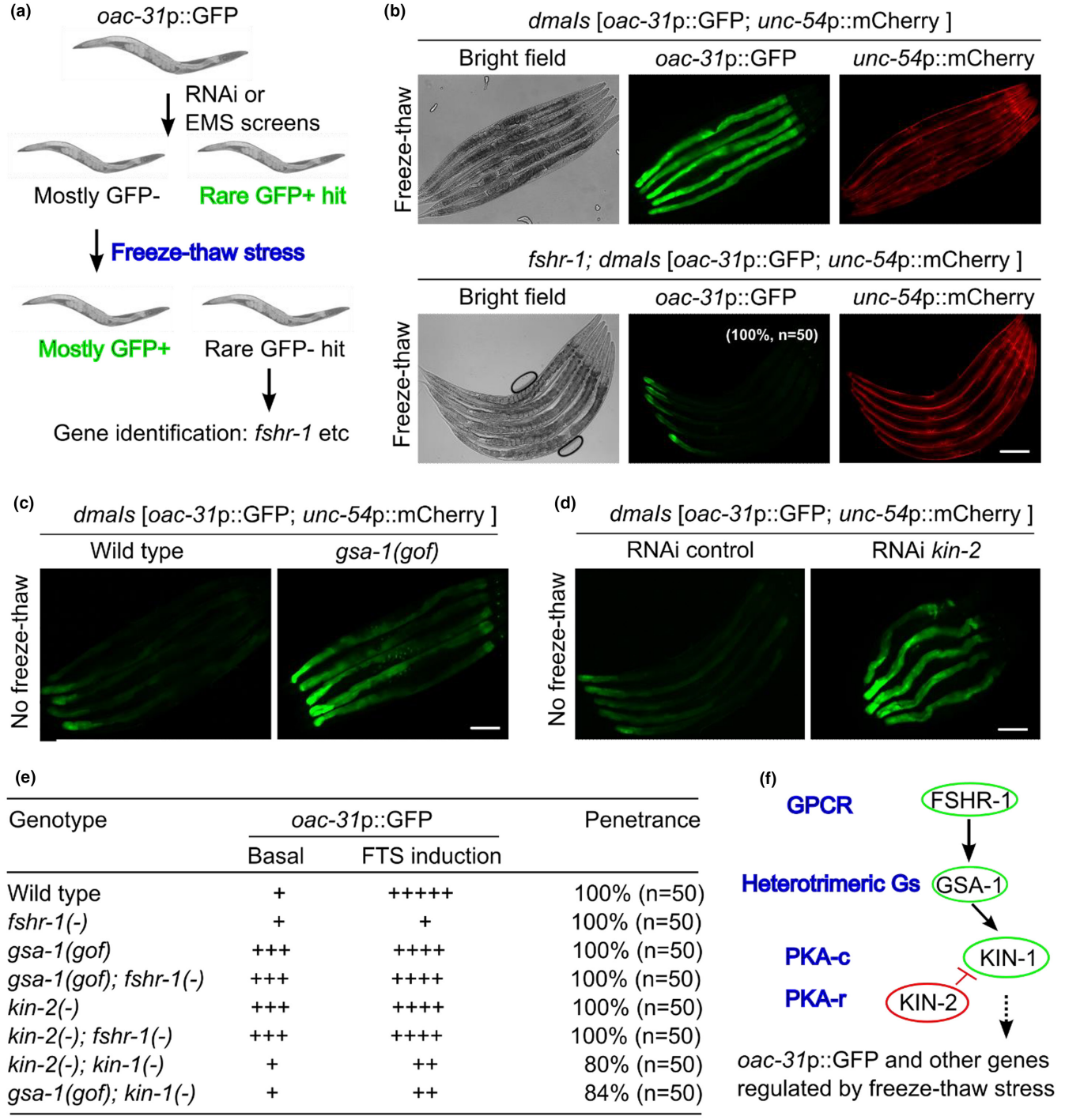

(e)

Genotype	*oac-31*p::GFP		Penetrance
	Basal	FTS induction	
Wild type	+	+++++	100% (n=50)
fshr-1(-)	+	+	100% (n=50)
gsa-1(gof)	+++	++++	100% (n=50)
gsa-1(gof); fshr-1(-)	+++	++++	100% (n=50)
kin-2(-)	+++	++++	100% (n=50)
kin-2(-); fshr-1(-)	+++	++++	100% (n=50)
kin-2(-); kin-1(-)	+	++	80% (n=50)
gsa-1(gof); kin-1(-)	+	++	84% (n=50)

FIGURE 2 Genetic screens identify FSHR-1/GPCR signaling in regulating freeze–thaw-induced *oac-31*. (a). Schematic of RNAi and EMS screens. (b), representative epifluorescence images showing FTS induction of *oac-31*p::GFP is blocked in *fshr-1* deletion mutants. (c), representative epifluorescence images showing constitutive induction of *oac-31*p::GFP in *gsa-1* gain-of-function mutants without FTS. (d), representative epifluorescence images showing constitutive induction of *oac-31*p::GFP in *kin-2* RNAi-treated animals without FTS. (e), summary table listing the *oac-31*p::GFP phenotype (with the numbers of "+" signs qualitatively indicating the GFP fluorescence levels) and penetrance of FTS induction in animals with genotypes indicated. (f), schematic of the FSHR-1/GSA/PKA pathway in regulating *oac-31* expression in response to FTS, based on genetic epistasis analysis. Scale bar, 100 μm

encoding a protease) decreased FTS-induced phenoptosis to a lesser extent (Figure 4b). These results indicate that FTS promotes phenoptosis through an FSHR-1/GSA-1/PKA/ZIP-10 cascade (Figure 4c).

FSHR-1 has been previously implicated in responses to oxidative and pathogen stresses (Miller et al., 2015, p.1; Powell et al., 2009, p.). Among the membrane lipids that can be oxidized, cholesterol is most prone to oxidation by reactive oxygen species (Murphy &

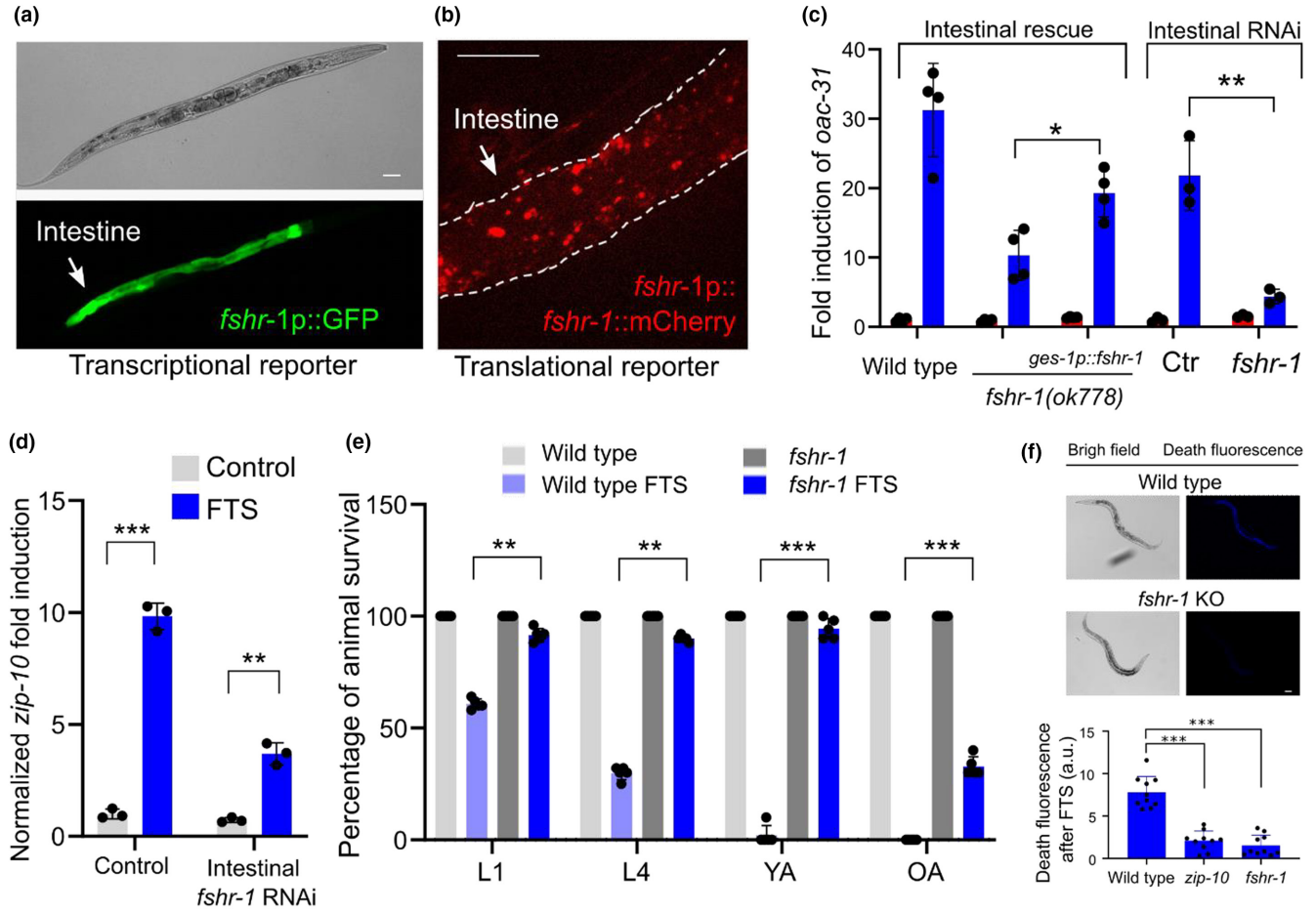

FIGURE 3 *Fshr-1* is expressed and acts in the intestine to regulate FTS induction of *oac-31* and phenoptosis. (a), representative epifluorescence image of the transcriptional *fshr-1*p::GFP reporter showing predominant expression of GFP in the intestine. (b), representative epifluorescence image of the translational *fshr-1*p::*Fshr-1*::mCherry reporter showing intestinal expression pattern. (c), tissue-specific rescue (*fshr-1* cDNA driven by the intestine-specific *ges-1* promoter) and *fshr-1* RNAi (in the strain *rde-1(ne219); is [Pges-1::rde-1::unc54 3′UTR; Pmyo-2::RFP]*) analysis showing *fshr-1* acting primarily in the intestine for FTS induction of *oac-31*. Values are means ± S.D with $^{**}p<0.01$ and $^{*}p<0.05$ (two-way ANOVA for genotype-effect interaction and post hoc Tukey HSD, N > 3 independent experiments, n > 50 for each experiment). (d), qRT-PCR results showing induction of *zip-10* by FTS was attenuated in animals with intestine-specific *fshr-1* RNAi. Values are means ± S.D with $^{**}p<0.01$, $^{***}p<0.001$ (two-way ANOVA for genotype-effect interaction and post hoc Tukey HSD, N = 3 independent experiments, n > 50 for each experiment). (e), quantification of phenoptosis based on percentages of larval (L1 and L4) and adult (YA: 48 h post L4, OA: 5 days post L4) stage animals survived after FTS treatment. Values are means ± S.D with $^{**}p<0.01$ and $^{***}p<0.001$ (two-way ANOVA for genotype-effect interaction and post hoc Tukey HSD, N > 3 independent experiments, n > 50 for each experiment). (f), representative bright field and fluorescence images showing characteristic blue "death fluorescence" in wild type but not *zip-10* or *fshr-1* mutants ($^{***}p<0.001$, one-way ANOVA with post hoc Tukey HSD, N = 10) 24 h after FTS. Scale bar, 100 μm

Johnson, 2008). Consistent with previous studies supporting the role of FSHR-1 in protecting against oxidative stress associated with cell membrane lipids, we found that *fshr-1* RNAi caused higher sensitivity than wild type to exposure to exogenous cholesterol when supplemented with the oxidizing agent Paraquat (Figure S3a). In addition, we found that the cold stress or FTS resilience phenotypes caused by RNAi against *fshr-1* can be modulated by the amount of exogenous (supplemented in media) or endogenous (manipulated by *ncr* expression) cholesterol availability (Figure S3b-d). These results suggest that resilience to severe hypothermic stress can come with a physiological trade-off in organismic resilience to cholesterol oxidative stress.

We next explored how FTS may regulate FLR-2/FSHR-1. Based on RNAseq results, FTS did not affect expression levels of *flr-2* or *fshr-1* (Figure S4a). While *flr-2* is expressed predominantly in neurons based on single-cell RNA results (Taylor et al., 2021), we generated a translational reporter for FLR-2 fused with GFP and identified its localization to coelomocytes, which likely uptake secreted forms of FLR-2::GFP from neurons (Figure S4b). However, *flr-2* reporters showed no apparent changes after FTS treatment (Figure S4b). These data suggest that neuron-derived systemically acting FLR-2 is required for FTS induction of *oac-31* and phenoptosis, but not directly regulated by FTS transcriptionally. Nonetheless, we observed

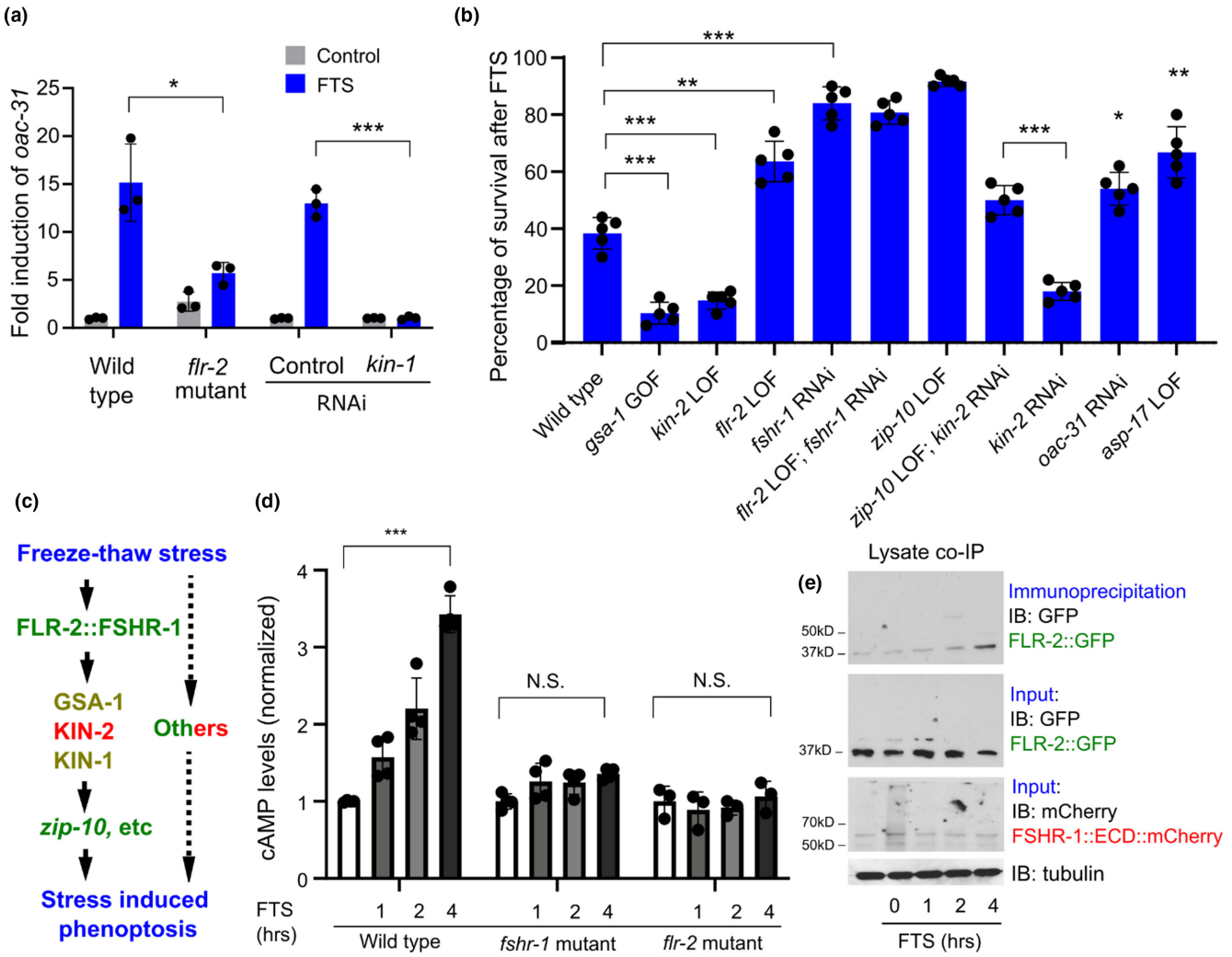

FIGURE 4 FLR-2/FSHR-1-mediated GPCR/cAMP signaling promotes phenoptosis. (a), qRT-PCR results showing abolished *oac-31* induction by FTS in *flr-2* reduction-of-function mutants, mimicking *fshr-1* mutants. $^{**}p<0.01$ (two-way ANOVA for genotype-effect interaction and post hoc Tukey HSD, N = 3 independent experiments, n > 50 for each experiment). (b), table summary of percentages of larval L4-stage animals with indicated genotypes survived after FTS treatment $^{*}p<0.05$ and $^{***}p<0.001$ (one-way ANOVA and post hoc Tukey HSD N = 5 independent experiments, n > 50 for each experiment). (c), schematic of the genetic pathway leading to FTS-induced phenoptosis based on epistasis and gene expression analysis. Known genes or proteins promoting (green) or antagonizing (red) cold stress-induced phenoptosis are noted and with other contributors (dashed line). (d), normalized ELISA results showing FTS-induced (no FTS control, 1 , 2 , 4 h of recovery after freezing) elevation of cAMP was abolished in *flr-2* and *fshr-1* mutants. Values are means ± S.D with $^{***}p<0.001$ (two-way ANOVA for genotype-effect interaction and post hoc Tukey HSD, N > 3 independent experiments, n > 50 for each experiment). N.S., non-significant. (e), representative western blots of GFP-tagged FLR-2, mCherry-tagged FSHR-1::ECD(extracellular domain)::mCherry from input and co-immunoprecipitation lysate samples showing time-dependent (no FTS control, 0, 1, 2, and 4 h of recovery after freezing) binding of FLR-2::GFP and FSHR-1::ECD::mCherry upon FTS treatment (tubulin as loading control)

that FTS induced marked elevation of intracellular cAMP levels in wild type but not *flr-2* or *fshr-1* mutants (Figure 4d). In addition, co-immunoprecipitation experiments using transgenic animals show that GFP-tagged FLR-2 can increasingly bind to mCherry-tagged FSHR-1 extracellular domains after FTS in a time-dependent manner (Figure 4e), consistent with an increase in cAMP levels after FTS. As glycoprotein hormones typically bind to its obligatory GPCRs to stimulate cAMP levels, these results further support the notion that FSHR-1-dependent GPCR signaling actively mediates the response to FTS, rather than plays a permissive role, to drive stress-induced gene expression and phenoptosis.

2.4 | A mathematical model to explain plausible adaptive functions of phenoptosis

At first glance, the existence of phenoptosis and a genetic pathway promoting phenoptosis would seem incompatible with classic evolutionary theory as genes promoting phenoptosis would compromise individual fitness, thus not being subject to selection pressure. Why would a genetic program possibly promote phenoptosis? We used a mathematical model (Figure 5) built upon the evolutionary concept of kin selection that may explain the adaptive or beneficial functions of phenoptosis at the population level. We define three key parameters

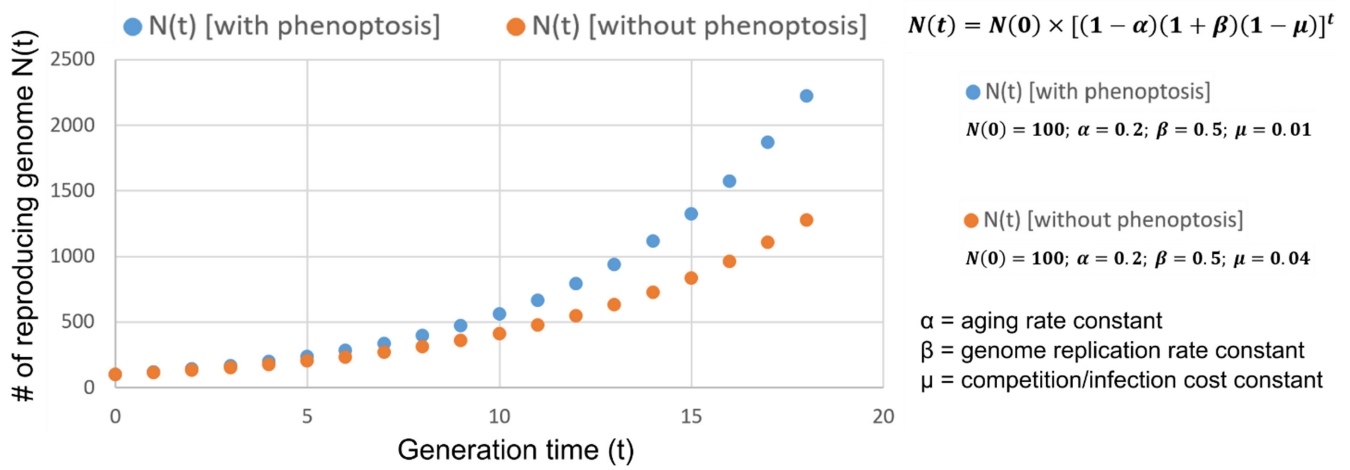

FIGURE 5 A simplified mathematical model to simulate the potential adaptive function of phenoptosis. Shown is a graph simulating the proliferation of reproducing genomes following the equation $N(t) = N(0) \times [(1-\alpha)(1+\beta)(1-\mu)]^t$, where N (0) = initial number of reproduction-competent haploid genomes in a population, N (t) = number of reproducing haploid genomes in a population at the generation time of t, α = aging rate constant, β = genome replication rate constant, μ = cohort competition/infection cost constant. For simulation, we used $N(0) = 100;\ \alpha = 0.2;\ \beta = 0.0;\ \mu = 0.04$ for the growth of numbers of reproducing genomes without phenoptosis or decreased phenoptosis (e.g. in *fshr-1* mutants), while $N(0) = 100;\ \alpha = 0.2;\ \beta = 0.5;\ \mu = 0.01$ with phenoptosis (e.g., in the wild-type *C. elegans*). For simplicity, we make assumptions on the clonal population structure and growth characteristics in a resource-limiting competitive environment and that α and β remain constant. Note that μ is lower with increased phenoptosis given limited resources for a population, since increased stress-induced phenoptosis in less reproduction-competent individuals leads to reduced competition for resources or vulnerability to pathogen infection at the population level

in the model that determine the growth of reproduction-competent haploid genomes in a population, including the parameter of α (aging rate), β (genome replication rate), and μ (cohort competition/infection cost after stress). More stress sensitivity (i.e., phenoptosis susceptible) in weak or old (vs. fit or young) animals would decrease μ, since weak or old animals contribute less than fit or young animals in the growth of replication-competent genomes in the population. Simulated results from our model assuming constant parameters in a given population show that the number of healthy individuals in a starting population can increase faster than a population without stress-inducible phenoptosis, under conditions where there is competition for limited resources to reproduce or infectious spreading of pathogens among individuals (Figure 5). According to the model, stress-induced phenoptosis may act against the unfit group members (severely stressed adults less reproductive or sick individuals shedding infectious pathogens) to benefit the whole group at the population level.

3 | DISCUSSION

While genes can control how cells die in well-known processes including apoptosis, necroptosis, and pyroptosis (Metzstein et al., 1998; Shi et al., 2017; Weinlich et al., 2017), how genes might control the death of an organism remains largely unclear. Based on comprehensive genetic analyses and stress-responding organismic phenotypes, we propose a model in which FSHR-1 signaling may mediate FTS-induced phenoptosis in *C. elegans*. After exposure to severe hypothermic stress conditions, FLR-2 may promote FSHR-1 activation and signaling through a GPCR-dependent Gαs-cAMP-PKA pathway, leading to increased expression of *zip-10*, *oac-31*, and other genes in a genetic program that coordinately regulate phenoptosis. Site-of-expression and site-of-action analyses indicate that this GPCR pathway operates in the intestine, consistent with intestinal expression and cell-autonomous regulation of *zip-10* and *oac-31*. Regarding the mechanism of how FTS activates FLR-2/FSHR-1, it is conceivable that sensory neurons may detect thermal stress signals to promote the release of FLR-2 to act systemically, while intestinal cells may also adjust membrane properties upon FTS to modulate FLR-2/FSHR-1 activation (Ernst et al., 2016). Although ZIP-10 is essential for up-regulation of many genes induced by FTS, mechanisms linking FSHR-1/GPCR, KIN-1/PKA to *zip-10* regulation remain unidentified. Candidate factors may include CREB/bZIP family transcription factors (Lakhina et al., 2015; Zhang et al., 2017, p.1) and the p38/JNK pathways (Hattori et al., 2013; Zhang et al., 2017). In particular, the stress-responding *kgb-1*/JNK pathway has been shown to promote detrimental effects during *C. elegans* aging (Twumasi-Boateng et al., 2012). Whether and how KGB-1 might play similar roles in FTS-induced phenoptosis remain to be investigated in future studies.

Various types of environmental stress other than FTS have been shown to trigger acute organismic death in *C. elegans* that is preceded by cellular necrosis in the intestine (Coburn et al., 2013; Ezcurra et al., 2018; Luke et al., 2007; Zhang et al., 2016). Mediators linking stress signals to cellular necrosis programs remain largely undefined and are likely stress type-specific. As ZIP-10 appears both

required and partially sufficient to drive cold-induced phenoptosis, it may represent a master transcriptional regulator downstream of stress-sensing GPCR signaling, leading to systemic necrosis and organismic death through its target gene effectors, including those encoding proteases we previously identified (Jiang et al., 2018). Our results suggest that the ISY-1/*mir-60* axis plays a gatekeeping role for ZIP-10 activation and phenoptosis, whereas the FLR-2/FSHR-1/GSA/KIN-2 axis is likely instructive by linking FTS to genes regulating cellular necrosis or promoting organismic sensitivity to lethal effects of FTS. It is worth noting that the death-promoting effect of PKA signaling after FTS differs from its protective effect under constitutive cold conditions (Liu et al., 2017), underscored by the fact that strong induction of the *zip-10* transcriptional program requires the warming or recovery phase post cold or freezing stresses (Jiang et al., 2018). FSHR-1 and ZIP-10 have also been shown to mediate host cell responses to oxidative stress, various types of pathogens and immune aging (Powell et al., 2009; Miller et al., 2015, p.1; Lee et al., 2021, p.1; Kato et al., 2016). Indeed, we found that *fshr-1* loss-of-function mutants, while being more FTS resistant than the wild type, were less tolerant of cholesterol oxidative stress (Figure S4). How FSHR-1/GPCR, KIN-1/PKA, or ZIP-10/bZIP may function in other stress paradigms similarly in promoting organismic phenoptosis or play context-specific roles in physiological trade-off awaits further studies.

We note that *oac-31*, like several other *oac* genes (*oac-3*, *6*, *14*, *20*) strongly up-regulated by FTS (Figure S1g), encodes a *C. elegans* homolog of sterol O-acyltransferase (SOAT). SOAT converts accessible cholesterol into ester forms for storage in lipid droplets (Luo et al., 2020; Sevanian & Peterson, 1986). While the biochemical function of OAC-31 remains further characterized, a recent study showed that cold shock can promote lipid movement from the intestine to the germline (Gulyas & Powell, 2021). Interestingly, the natural aging of *C. elegans* is accompanied with autophagy-mediated conversion of intestinal biomass into the yolk, contributing to late-life aging pathologies and mortality (Ezcurra et al., 2018). Thus, it is plausible that FSHR-1-dependent up-regulation of SOAT may be part of a genetic program that converts somatic biomass into nutrient/energy reserves for trafficking to the germline to benefit the progeny at the expense of parental death. In early life, such genetic programs may have evolved to promote reproductive health, while exhibiting antagonistic pleiotropic effects promoting organismic death and aging in late life. Phenoptosis-promoting effects of FSHR-1/ZIP-10 are also dependent on developmental stages, stress types, and severity, reflecting on their pleiotropic context-dependent nature. At the population level, the phenoptosis of severely stressed weak or sick adults (aged or infected) may also be beneficial as limiting resources can be funneled to less severely stressed and reproductively active younger individuals. These two scenarios ("disposable soma" and "kin selection") are not mutually exclusive and may have been subject to selection pressure and explain the conservation of phenoptosis and its pathway of regulation in certain species, particularly those with clonal population structures (Galimov et al., 2019). Together, our findings identify key signaling mediators of severe cold stress-induced phenoptosis in *C. elegans* and provide empirical evidence of how phenoptosis can be genetically regulated with plausible evolutionary significance.

4 | MATERIALS AND METHODS

4.1 | *C. elegans* strains

C. elegans strains were maintained with standard procedures unless otherwise specified. The N2 Bristol strain was used as the reference wild type, and the polymorphic Hawaiian strain CB4856 was used for genetic linkage mapping and SNP analysis (Brenner, 1974; Davis et al., 2005). A forward genetic screen for *oac-31*p::GFP mutants after ethyl methanesulfonate (EMS)-induced random mutagenesis was performed as described previously (Ma et al., 2012; Ma et al., 2015). Feeding RNAi was performed as previously described (Kamath & Ahringer, 2003). Customized sub-libraries of RNAi, clones were constructed by manual selection from the main Ahringer library based on gene expression abundance (TPM > 2) in the intestine and encoded proteins as putative transmembrane receptors, signaling proteins, and transcription factors (Table S1). Transgenic strains were generated by germline transformation as described (Mello et al., 1991). Transgenic constructs were co-injected (at 10–50 ng/μl) with dominant *unc-54p*::mCherry or *rol-6* markers, and stable extrachromosomal lines of mCherry+ or roller animals were established. Genotypes of strains used are: *gsa-1(ce81) I*, *ncr-2(nr2023) III*, *fshr-1(ok778) V*, *flr-2(ut5) V*, *ncr-1(nr2022) X*. *dmaEx616 [fshr-1p::GFP; unc-54p::mCherry]*, *vjEx1449[ges-1p::fshr-1]*, *dmaEx617 [fshr-1p::fshr-1::GFP; unc-54p::mCherry]*, *dmaEx620 [rpl-28p::fshr-1ECD::mCherry]*, *rde-1(ne219)*; *Is[Pges-1::rde-1::unc54 3′UTR; Pmyo-2::RFP3]* (gift of Dr. Meng Wang's laboratory), *dmaIs136 [flr-2p::flr-2::GFP]*, *dmaIs117 IV [oac-31p::GFP; unc-54p::mCherry]*.

4.2 | Sample preparation for RNA sequencing and data analysis

Control N2 animals were maintained at 20 °C. For freeze–thaw stress, N2 animals were exposed to −20 °C for 25 min followed by 1 h recovery at 20 °C. Upon sample collection, the animals were washed down from NGM plates using M9 solution and subjected to RNA extraction using the RNeasy Mini Kit from Qiagen. 1 μg total RNA from each sample was used for sequencing library construction. RNA-seq Library preparation and data analysis were performed as previously described (Jiang et al., 2018). Three biological replicates were included for each treatment. The libraries were sequenced to 51 bp at the single end by the Center for Advanced Technology (CAT) of the University of California, San Francisco, using a Hiseq-3000 system. The cleaned RNAseq reads were mapped to the genome sequence of *C. elegans* using hisat2 (Kim et al., 2015). The mapped reads were assigned to the genes using featureCounts (Liao et al., 2014). The abundance of genes

was expressed as RPKM (Reads per kilobase per million mapped reads). Identification of differentially expressed genes was performed using the DESeq2 package (Love et al., 2014).

4.3 | Quantitative RT-PCR

25 μl pellet animals were resuspended in 400 μl lysis buffer of Quick-RNA MiniPrep kit (Zymo Research, R1055) then lysed by TissueRuptor (Motor unit "8" for 1 min). Total RNA was extracted following the instruction (Zymo Research, R1055). 1 μg RNA/sample was reverse transcribed into cDNA (Thermo Fisher Scientific, 18080051). Real-time PCR was performed by using Roche LightCycler96 (Roche, 05815916001) system and SYBR Green (Thermo Fisher Scientific, FERK1081) as a dsDNA-specific binding dye. The qRT-PCR condition was set to 95 °C for denaturation, followed by 45 cycles of 10 s at 95 °C, 10 s at 60 °C, and 20 s at 72 °C. Melting curve analysis was performed after the final cycle to examine the specificity of primers in each reaction. Relative mRNA was calculated by ΔΔCT method and normalized to actin. Primers for qRT-PCR: *oac-31* (Forward, ATGGCTTAAATCGCTGGAAA; Reverse, ATCTTTCGCCATCAATACGG), *W09G12.7*, (Forward, CGAAGATCACTCGAACACGA; Reverse, CCATTTTTACGAAGG CTGGA), *tsp-1* (Forward, CTTTGATTGCCGTTGGATTT; Reverse, CCCAAAGAAAGGCCGATAAT), *act-3* (Forward, TCCATCATGAAGTGCGACAT; Reverse, TAGATCCTCCGATCC AGACG).

4.4 | Freezing resilience assay

Animals were cultured under non-starved conditions for at least 4 generations at 20 °C before cold and freezing resilience assay. For freezing resilience assay, bleach-synchronized L1, L4, young (48 h post L4), and older adult (5 days post L4) populations were kept at −20 °C for 45 min and then recovered for 24 h at 20 °C. For such experiments, NGM plates spread with equal agar thickness seeded with equal amounts of OP50 were used while hypothermic temperature readings were monitored by thermometers to ensure minimal fluctuation. After freezing shock, animals were moved to 20 °C for recovery and scored as dead if they showed no pumping and movement upon light touch with the body necrosis subsequently confirmed.

4.5 | cAMP assay

N2, *fshr-1*, and *flr-2* mutants were freeze-shocked (−20 °C) for 25 min, followed by recovery at 20 °C for 0, 1, 2, or 4 h. Animals were harvested and washed three times with M9 and 20 μl, pellet animals were lysed directly in ELISA lysis buffer. Then, worm extracts were collected by centrifugation. The cAMP levels in the supernatant were determined using the cyclic AMP ELISA kit (Cayman Chemical) according to the manufacturer's instructions. A BCA kit was used to measure the concentration of protein as a normalizing control.

4.6 | Co-immunoprecipitation assay

Transgenic animals expressing *flr-2p::flr-2::GFP* and *fshr-1::ECD::mcherry* were cultured under non-starved conditions at 20 °C on NGM plates before freezing treatment. For freezing treatment, mixed-stage worms were kept at −20 °C for 25 min and then recovery for 0, 1, 2, and 4 h at 20 °C. Upon sample collection, the animals were washed down from NGM plates using M9 solution and subjected to protein extraction using ice-cold 2x lysis buffer (60 mM HEPES, pH = 7.4, 100 mM potassium chloride, 0.1% Triton X, 4 mM magnesium chloride, 10% glycerol, 2 mM DTT with RNase inhibitor, protease inhibitor, and phosphatase inhibitors) and lysed with sonication. The lysate was then centrifuged at 15,000 rpm for 15 min to remove cell debris. The supernatant was incubated with 4 μl of pre-clean magnetic beads at 4 °C for 15 min. To precipitate *fshr-1*::ECD::mcherry proteins, the sample was placed into a 1.5 ml RNase-free tube containing RFP-trap magnetic beads at 4 °C overnight. The beads were then washed with 400 μl of lysis buffer for 5 times and incubated with *flr-2::flr-2::GFP* lysate samples at 4 °C overnight. The beads were then washed with 400 μl of lysis buffer 5 times and resuspended in 40 μl of 1× Laemmli Sample Buffer. The samples were then boiled at 95 °C for 10 min and subjected to Western blot analysis.

4.7 | Statistical analysis

Data were analyzed using GraphPad Prism 9.2.0 Software (Graphpad) and presented as means ± S.D. unless otherwise specified, with *P* values calculated by unpaired two-tailed t-tests (comparisons between two groups), one-way or two-way ANOVA (comparisons across more than two groups) followed by Tukey's post hoc tests and adjusted with Bonferroni's corrections.

AUTHOR CONTRIBUTIONS

C.W., B.W., C.Z., and D.K.M. designed, performed, and analyzed the experiments and wrote the manuscript. Y.L. performed RNA sequencing and analysis. C.Z. and D.K.M. provided resources and supervised the project.

ACKNOWLEDGMENTS

Some strains were provided by the CGC, which is funded by the NIH Office of Research Infrastructure Programs (P40 OD010440), and from Drs. Derek Sieburth and Meng Wang laboratories. The work was supported by NIH grant 1R35GM139618 and the Packard Fellowship in Science and Engineering (D.K.M) and National Natural Science Foundation of China, Grant No. 32271165, 31971077, and 31971047 (C.Z., C.W.).

CONFLICT OF INTEREST

The authors declare no competing interests.

DATA AVAILABILITY STATEMENT

The RNAseq read datasets were deposited in NCBI SRA (Sequence Read Archive) under the BioProject accession PRJNA763790. All other data newly generated for this study are included in this article.

ORCID

Dengke K. Ma https://orcid.org/0000-0002-5619-7485

REFERENCES

Al-Fageeh, M. B., & Smales, C. M. (2006). Control and regulation of the cellular responses to cold shock: The responses in yeast and mammalian systems. *The Biochemical Journal*, *397*, 247–259.

Antebi, A. (2007). Genetics of aging in Caenorhabditis elegans. *PLoS Genetics*, *3*, 1565–1571.

Brenner, S. (1974). The genetics of Caenorhabditis elegans. *Genetics*, *77*, 71–94.

Cho, S., Rogers, K. W., & Fay, D. S. (2007). The C. elegans glycopeptide hormone receptor ortholog, FSHR-1, regulates germline differentiation and survival. *Current Biology*, *17*, 203–212.

Coburn, C., Allman, E., Mahanti, P., Benedetto, A., Cabreiro, F., Pincus, Z., Matthijssens, F., Araiz, C., Mandel, A., Vlachos, M., Edwards, S.-A., Fischer, G., Davidson, A., Pryor, R. E., Stevens, A., Slack, F. J., Tavernarakis, N., Braeckman, B. P., Schroeder, F. C., … Gems, D. (2013). Anthranilate fluorescence Marks a calcium-propagated necrotic wave that promotes organismal death in C. elegans. *PLoS Biology*, *11*, e1001613.

Davis, M. W., Hammarlund, M., Harrach, T., Hullett, P., Olsen, S., & Jorgensen, E. M. (2005). Rapid single nucleotide polymorphism mapping in C. elegans. *BMC Genomics*, *6*, 118.

Ernst, R., Ejsing, C. S., & Antonny, B. (2016). Homeoviscous adaptation and the regulation of membrane lipids. *Journal of Molecular Biology*, *428*, 4776–4791.

Ezcurra, M., Benedetto, A., Sornda, T., Gilliat, A. F., Au, C., Zhang, Q., van Schelt, S., Petrache, A. L., Wang, H., de la Guardia, Y., Bar-Nun, S., Tyler, E., Wakelam, M. J., & Gems, D. (2018). C. elegans eats its own intestine to make yolk leading to multiple senescent pathologies. *Curr. Biol. CB*, *28*, 2544–2556.e5.

Fontana, L., & Partridge, L. (2015). Promoting health and longevity through diet: From model organisms to humans. *Cell*, *161*, 106–118.

Galimov, E. R., & Gems, D. (2020). Shorter life and reduced fecundity can increase colony fitness in virtual Caenorhabditis elegans. *Aging Cell*, *19*, e13141.

Galimov, E. R., Lohr, J. N., & Gems, D. (2019). When and how can death Be an adaptation? *Biochemistry Biokhimiia*, *84*, 1433–1437.

Garrity, P. A., Goodman, M. B., Samuel, A. D., & Sengupta, P. (2010). Running hot and cold: Behavioral strategies, neural circuits, and the molecular machinery for thermotaxis in C. elegans and drosophila. *Genes & Development*, *24*, 2365–2382.

Gulyas L & Powell JR (2021) *Cold shock induces a terminal investment reproductive response in C. elegans*. Accessed October 8, 2021. https://www.biorxiv.org/content/10.1101/2021.09.11.459896v1

Hamilton, W. D. (1963). The evolution of altruistic behavior. *The American Naturalist*, *97*, 354–356.

Hattori, A., Mizuno, T., Akamatsu, M., Hisamoto, N., & Matsumoto, K. (2013). The Caenorhabditis elegans JNK signaling pathway activates expression of stress response genes by derepressing the Fos/HDAC repressor complex. *PLoS Genetics*, *9*, e1003315.

Jiang, W., Wei, Y., Long, Y., Owen, A., Wang, B., Wu, X., Luo, S., Dang, Y., & Ma, D. K. (2018). A genetic program mediates cold-warming response and promotes stress-induced phenoptosis in C. elegans. *eLife*, *7*, e35037.

Kamath, R. S., & Ahringer, J. (2003). Genome-wide RNAi screening in Caenorhabditis elegans. *Methods San Diego Calif*, *30*, 313–321.

Kato, M., Kashem, M. A., & Cheng, C. (2016). An intestinal microRNA modulates the homeostatic adaptation to chronic oxidative stress in C. elegans. *Aging*, *8*, 1979–2005.

Kenyon, C. J. (2010). The genetics of ageing. *Nature*, *464*, 504–512.

Kim, D., Langmead, B., & Salzberg, S. L. (2015). HISAT: A fast spliced aligner with low memory requirements. *Nature Methods*, *12*, 357–360.

Kim, S., & Sieburth, D. (2020). FSHR-1/GPCR regulates the mitochondrial unfolded protein response in Caenorhabditis elegans. *Genetics*, *214*, 409–418.

Kirkwood, T. B. L., & Melov, S. (2011). On the programmed/non-programmed nature of ageing within the life history. *Current Biology CB*, *21*, R701–R707.

Kudo, M., Chen, T., Nakabayashi, K., Hsu, S. Y., & Hsueh, A. J. (2000). The nematode leucine-rich repeat-containing, G protein-coupled receptor (LGR) protein homologous to vertebrate gonadotropin and thyrotropin receptors is constitutively active in mammalian cells. *Molecular endocrinology (Baltimore, Md.)*, *14*, 272–284.

Lakhina, V., Arey, R. N., Kaletsky, R., Kauffman, A., Stein, G., Keyes, W., Xu, D., & Murphy, C. T. (2015). Genome-wide functional analysis of CREB/Long-term memory-dependent transcription reveals distinct basal and memory gene expression programs. *Neuron*, *85*, 330–345.

Lee, D., An, S. W. A., Jung, Y., Yamaoka, Y., Ryu, Y., Goh, G. Y. S., Beigi, A., Yang, J.-S., Jung, G. Y., Ma, D. K., Ha, C. M., Taubert, S., Lee, Y., & Lee, S.-J. V. (2019). MDT-15/MED15 permits longevity at low temperature via enhancing lipidostasis and proteostasis. *PLoS Biology*, *17*, e3000415.

Lee, Y., Jung, Y., Jeong, D.-E., Hwang, W., Ham, S., Park, H.-E. H., Kwon, S., Ashraf, J. M., Murphy, C. T., & Lee, S.-J. V. (2021). Reduced insulin/IGF1 signaling prevents immune aging via ZIP-10/bZIP-mediated feedforward loop. *The Journal of Cell Biology*, *220*, e202006174.

Liao, Y., Smyth, G. K., & Shi, W. (2014). featureCounts: An efficient general purpose program for assigning sequence reads to genomic features. *Bioinformatics Oxford England*, *30*, 923–930.

Liu, F., Xiao, Y., Ji, X.-L., Zhang, K.-Q., & Zou, C.-G. (2017). The cAMP-PKA pathway-mediated fat mobilization is required for cold tolerance in C. elegans. *Scientific Reports*, *7*, 638.

Longo, V. D., Mitteldorf, J., & Skulachev, V. P. (2005). Programmed and altruistic ageing. *Nature Reviews Genetics*, *6*, 866–872.

López-Otín, C., Blasco, M. A., Partridge, L., Serrano, M., & Kroemer, G. (2013). The hallmarks of aging. *Cell*, *153*, 1194–1217.

Love, M. I., Huber, W., & Anders, S. (2014). Moderated estimation of fold change and dispersion for RNA-seq data with DESeq2. *Genome Biology*, *15*, 550.

Lu, X. Y., Gross, R. E., Bagchi, S., & Rubin, C. S. (1990). Cloning, structure, and expression of the gene for a novel regulatory subunit of cAMP-dependent protein kinase in Caenorhabditis elegans. *The Journal of Biological Chemistry*, *265*, 3293–3303.

Luke, C. J., Pak, S. C., Askew, Y. S., Naviglia, T. L., Askew, D. J., Nobar, S. M., Vetica, A. C., Long, O. S., Watkins, S. C., Stolz, D. B., Barstead, R. J., Moulder, G. L., Brömme, D., & Silverman, G. A. (2007). An intracellular serpin regulates necrosis by inhibiting the induction and sequelae of lysosomal injury. *Cell*, *130*, 1108–1119.

Luo, J., Yang, H., & Song, B.-L. (2020). Mechanisms and regulation of cholesterol homeostasis. *Nature Reviews Molecular Cell Biology*, *21*, 225–245.

Ma, D. K., Li, Z., Lu, A. Y., Sun, F., Chen, S., Rothe, M., Menzel, R., Sun, F., & Horvitz, H. R. (2015). Acyl-CoA dehydrogenase drives heat adaptation by sequestering fatty acids. *Cell*, *161*, 1152–1163.

Ma, D. K., Vozdek, R., Bhatla, N., & Horvitz, H. R. (2012). CYSL-1 interacts with the O2-sensing hydroxylase EGL-9 to promote H2S-modulated hypoxia-induced behavioral plasticity in C. elegans. *Neuron*, *73*, 925–940.

Mello, C. C., Kramer, J. M., Stinchcomb, D., & Ambros, V. (1991). Efficient gene transfer in C.elegans: Extrachromosomal maintenance and integration of transforming sequences. *The EMBO Journal*, *10*, 3959–3970.

Metzstein, M. M., Stanfield, G. M., & Horvitz, H. R. (1998). Genetics of programmed cell death in C. elegans: Past, present and future. *Trends in Genetics*, *14*, 410–416.

Miller, E. V., Grandi, L. N., Giannini, J. A., Robinson, J. D., & Powell, J. R. (2015). The conserved G-protein coupled receptor FSHR-1 regulates protective host responses to infection and oxidative stress. *PLoS One*, *10*, e0137403.

Murphy, R. C., & Johnson, K. M. (2008). Cholesterol, reactive oxygen species, and the formation of biologically active mediators. *The Journal of Biological Chemistry*, *283*, 15521–15525.

Mutlu, A. S., Duffy, J., & Wang, M. C. (2021). Lipid metabolism and lipid signals in aging and longevity. *Developmental Cell*, *56*, 1394–1407.

Oishi, A., Gengyo-Ando, K., Mitani, S., Mohri-Shiomi, A., Kimura, K. D., Ishihara, T., & Katsura, I. (2009). FLR-2, the glycoprotein hormone alpha subunit, is involved in the neural control of intestinal functions in Caenorhabditis elegans. *Genes to Cells: Devoted to Molecular & Cellular Mechanisms*, *14*, 1141–1154.

Powell, J. R., Kim, D. H., & Ausubel, F. M. (2009). The G protein-coupled receptor FSHR-1 is required for the Caenorhabditis elegans innate immune response. *Proceedings of the National Academy of Sciences of the United States of America*, *106*, 2782–2787.

Sapolsky, R. M. (2004). *Why zebras Don't get ulcers* (3rd ed.). Holt Paperbacks.

Schade, M. A., Reynolds, N. K., Dollins, C. M., & Miller, K. G. (2005). Mutations that rescue the paralysis of Caenorhabditis elegans ric-8 (synembryn) mutants activate the G alpha(s) pathway and define a third major branch of the synaptic signaling network. *Genetics*, *169*, 631–649.

Sevanian, A., & Peterson, A. R. (1986). The cytotoxic and mutagenic properties of cholesterol oxidation products. *Food and Chemical Toxicology: An International Journal Published for the British Industrial Biological Research Association*, *24*, 1103–1110.

Shi, J., Gao, W., & Shao, F. (2017). Pyroptosis: Gasdermin-mediated programmed necrotic cell death. *Trends in Biochemical Sciences*, *42*, 245–254.

Shore, D. E., & Ruvkun, G. (2013). A cytoprotective perspective on longevity regulation. *Trends in Cell Biology*, *23*, 409–420.

Skulachev, V. P. (1999). Phenoptosis: Programmed death of an organism. *Biochemistry Biokhimiia*, *64*, 1418–1426.

Skulachev, V. P. (2002). Programmed death phenomena: From organelle to organism. *Annals of the New York Academy of Sciences*, *959*, 214–237.

Skulachev, V. P. (2019). Phenoptosis as a phenomenon widespread among many groups of living organisms including mammals (commentary to the paper by E. R. Galimov, J. N. Lohr, and D. Gems (2019) biochemistry (Moscow), 84, 1433-1437). *Biochemistry Biokhimiia*, *84*, 1438–1441.

Smith, J. M. (1964). Group selection and kin selection. *Nature*, *201*, 1145–1147.

Taylor, S. R., Santpere, G., Weinreb, A., Barrett, A., Reilly, M. B., Xu, C., Varol, E., Oikonomou, P., Glenwinkel, L., McWhirter, R., Poff, A., Basavaraju, M., Rafi, I., Yemini, E., Cook, S. J., Abrams, A., Vidal, B., Cros, C., Tavazoie, S., … Miller, D. M. (2021). Molecular topography of an entire nervous system. *Cell*, *184*, 4329–4347.e23.

Twumasi-Boateng, K., Wang, T. W., Tsai, L., Lee, K.-H., Salehpour, A., Bhat, S., Tan, M.-W., & Shapira, M. (2012). An age-dependent reversal in the protective capacities of JNK signaling shortens Caenorhabditis elegans lifespan. *Aging Cell*, *11*, 659–667.

Weinlich, R., Oberst, A., Beere, H. M., & Green, D. R. (2017). Necroptosis in development, inflammation and disease. *Nature Reviews Molecular Cell Biology*, *18*, 127–136.

Wu, D., Wang, Z., Huang, J., Huang, L., Zhang, S., Zhao, R., Li, W., Chen, D., & Ou, G. (2022). An antagonistic pleiotropic gene regulates the reproduction and longevity tradeoff. *Proceedings of the National Academy of Sciences of the United States of America*, *119*, e2120311119.

Xiao, R., Zhang, B., Dong, Y., Gong, J., Xu, T., Liu, J., & Xu, X. Z. S. (2013). A genetic program promotes C. elegans longevity at cold temperatures via a thermosensitive TRP channel. *Cell*, *152*, 806–817.

Zhang, F., Peng, D., Cheng, C., Zhou, W., Ju, S., Wan, D., Yu, Z., Shi, J., Deng, Y., Wang, F., Ye, X., Hu, Z., Lin, J., Ruan, L., & Sun, M. (2016). Bacillus thuringiensis crystal protein Cry6Aa triggers Caenorhabditis elegans necrosis pathway mediated by aspartic protease (ASP-1). *PLoS Pathogens*, *12*, e1005389.

Zhang, Z., Liu, L., Twumasi-Boateng, K., Block, D. H. S., & Shapira, M. (2017). FOS-1 functions as a transcriptional activator downstream of the C. elegans JNK homolog KGB-1. *Cellular Signalling*, *30*, 1–8.

SUPPORTING INFORMATION

Additional supporting information can be found online in the Supporting Information section at the end of this article.

How to cite this article: Wang, C., Long, Y., Wang, B., Zhang, C., & Ma, D. K. (2023). GPCR signaling regulates severe stress-induced organismic death in *C. elegans*. *Aging Cell*, *22*, e13735. https://doi.org/10.1111/acel.13735